

SMALL STRAIN MEASUREMENT

USING MODIFIED LDTs

Dasari, G.R., Bolton, M.D. and Ng, C.W.W.N.

CUED/D-SOILS/TR275 (1995)

SMALL STRAIN MEASUREMENT USING MODIFIED LDTs

Synopsis

Measurement of small strain stiffness of soils is fundamental to the understanding of the mechanics of soil particles since it allows to compare the properties obtained from dynamic and static tests. Local deformation transducers (LDTs) were developed to measure axial strains internally on triaxial samples. The resolution and the accuracy of LDTs is discussed. The LDTs were used to measure small strain stiffness of Gault Clay and results from a triaxial test are presented.

1.1 Introduction

Recent research has highlighted the importance of small strain measurement to evaluate the pre-failure stress-strain behaviour of soils (Simpson et al., 1979; Jardine et al., 1986; Stallebrass, 1990; Simpson, 1992; Bolton et al., 1993; Bolton et al., 1994). For example, prediction of ground movements behind a diaphragm wall demands correct stiffness of soil at small strains. Various types of dynamic tests have been developed for measuring the stiffness of soils at relatively small strains. They may be divided into (a) wave propagation methods such as ultra-sonic pulse and bender elements (Lacasse and Berre, 1988; Dyvik and Oslen, 1989; Viggiani, 1992) and (b) vibration methods such as resonant-column (RC) test (Taylor and Parton, 1974; Hardin and Drevenich, 1972). In spite of their popularity, the current dynamic tests have following limitations:

- 1) The maximum applicable strain is rather small. For instance, it is usually not larger than 0.1% in RC tests and about 10^{-4} to 10^{-6} % in wave propagation methods.
- 2) It is nearly impossible to control the strain rate in both types of methods. For example, the strain rate in RC tests is too large for most geotechnical engineering problems.

Most of the static tests do not have above limitations but there are other potential errors (e.g., piston friction for determining axial stress and bedding error for measuring axial strain in triaxial tests). If these problems could be eliminated by measuring the axial stress and axial strain locally, strength and deformation characteristics of soils can be investigated for any given stress path at a given strain rate by static tests. Though there is strong evidence that stiffness determined from static and dynamic tests seem to be close (Viggiani, 1992; Lefebvre et al., 1994; Clayton et al., 1994; Yasuda and Matsumoto, 1994), uncertainties do exist where the difference was attributed to visco-elastic properties of clay, Abbiss (1981). The principal sources of error in the external measurement of axial strain using LVDTs have been identified, among others, by Baldi et al. (1988) and are shown in Fig.1.1. The errors in external measurement of axial strain consist compliance of load measuring system, sample bedding effects, minor leakages and presence of air bubbles in the system. Although the errors due to compliance of the system can be evaluated with careful calibration, or modifications can be made to the apparatus to increase its stiffness (Kokush, 1980), other errors can be very difficult to assess.

The errors due to both compliance of the system and bedding can be eliminated by measuring axial strain of soil sample over a gauge length of soil sample. A large number of methods have been proposed to measure strains locally in a triaxial sample. They include displacement transducers (LVDTs) directly attached to the soil sample (Brown et al., 1980; Costa-Filho, 1985), X-ray and optical methods (Balasubramanian, 1976; Arthur and Phillips, 1975), proximity transducers (Hird and Yung, 1989), Imperial College strain gauges in both the original electrolevel and the new pendulum inclinometer designs (Burland and Symes,

1982; Jardine et al., 1984), Hall effect transducers (Clayton and Kathrush, 1986; Clayton et al., 1989) and thin strips of phosphor bronze (Local Deformation Transducers, LDTs) with strain gauges attached (Goto et al., 1991). The resolution and accuracy of the different types of transducers vary but measurement using LDTs seems to be easy and cheap. A modified version of LDTs similar to the ones used by Goto et al. (1991) were developed to measure small strains in triaxial system. The working principle of LDT is very simple. As the soil sample deforms, the distance between the two hinges changes and the curvature of the LDT. Strain gauges fixed at the centre of the LDT measure the bending strain in terms of voltage. Initial calibration of bending strain (voltage) versus axial strain is used to evaluate the axial strain. The axial strain of soil sample is the average of two LDTs placed right opposite to each other.

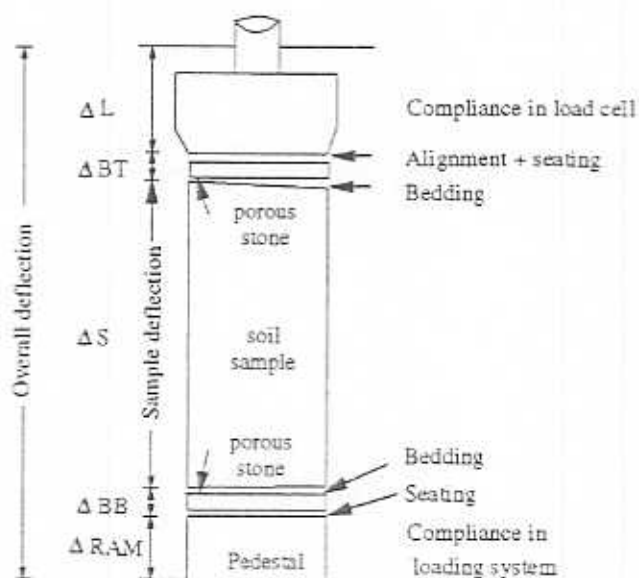


Fig. 1.1 Sources of error in conventional measurement of axial strain in triaxial testing (after Baldi et al., 1988)

1.2 Cambridge Triaxial Set-Up

The existing triaxial set-up was fully modified to add state-of-the-art features like computer controlled digital controllers (one each for lower chamber, cell pressure and pore pressure/back pressure), extension cap and small strain measuring device. Modified version of GDS software, called TRISP (Triaxial Stress Path) capable of logging data from 8 more channels, was installed on a new IBM PC with a CIL 16-bit A/D super card. The development of various new features is described in the following sections.

1.2.1 Junction box and data logging

A dedicated junction box with 8 channels was added to the set-up. Signal lines from load cell, LVDTs and LDTs were connected to a junction box (one channel for load cell, two channels for two LVDTs and two more channels for LDTs). Table 1 shows the configured arrangement of transducers connected to the junction box. The Junction box had an amplifier and a 1.6 kHz general purpose filter. The amplifier could amplify signals by 1, 10, 100 or 1000 times. The output from the junction box was sent to a 16 bit A/D card on an IBM PC. The A/D converter card had three input voltage ranges ± 100 mV, ± 1 V and ± 10 V. Table 1

also shows the voltage range on A/D card adopted for various transducers. A digital filter of F200 for LDTs and F20 for load cell and LVDTs was used to log the data. In F200, a single output voltage is the average of 200 readings which are continuously logged on at an interval of 2 mS. Use of F200 for LDTs has an advantage of reducing the noise of signal but at the expense of time. But for a static test, like the one planned, the time taken for F200 (400 mS for each channel) is not critical. There are 3 additional channels available on junction box to add some more facilities like mid plane PPT, radial strain measurement etc.

Table 1 The configured arrangement of transducers on junction box

| | Purpose | Input Voltage | Amplification | Voltage on A/D card | Filter |
|-----------|---------------|---------------|---------------|---------------------|--------|
| Channel 1 | Load Cell | $\pm 2V$ | 100 | $\pm 1V$ | F200 |
| Channel 2 | LDT1 | $\pm 2V$ | 100 | $\pm 1V$ | F200 |
| Channel 3 | LDT2 | $\pm 5V$ | 100 | $\pm 1V$ | F20 |
| Channel 4 | Radial strain | not | yet | implemented | |
| Channel 5 | Mid PPT | not | yet | implemented | |
| Channel 6 | End PPT | not | yet | implemented | |
| Channel 7 | LVDT1 | $\pm 5V$ | 1 | $\pm 10V$ | F20 |
| Channel 8 | LVDT2 | $\pm 5V$ | 1 | $\pm 10V$ | F20 |

1.2.2 Development of hinges

Hinges are used to connect the Local deformation Transducers (LDTs) to the soil sample. The inside corners of the hinges were made circular (radius 0.125mm) so that LDTs ends can fit exactly, Fig. 1.2 (a). Hinges were made up of light dural material. Hinges were glued to the membrane of the soil sample with super glue.

1.2.3 Development and Modifications of LDT

Initially an attempt was made to use the original design of the LDT by Goto et al., 1991. However, two problems were soon encountered. Firstly, the coating applied on the strain gauges was "over-cooked" because the gauge area was insufficient to dissipate the heat developed in to the surrounding static water in triaxial cell. Secondly, there was lack of fit at the reception corner of the hinge attachment. This could significantly affect the accuracy of the measurement.

There were three options to rectify the former problem: (a) to decrease the energisation voltage (b) to increase the gauge area and (c) to increase the resistance. The first option was considered to be inappropriate as decreasing the energisation voltage would have further reduced the output voltage. Second option was not possible because there were no strain gauges available with more gauge area but having same resistance. Hence, it was decided to follow option (c) by using eight strain gauges, four on each side of the strip, to form a full Wheatstone bridge as shown in Fig. 1.2 (c). In this way the current flow through each strain gauge is halved as the resistance is doubled. Since the heat generation is proportional to the product of current squared times the resistance, the amount of heat generated in each arm is effectively halved. The heat generated for unit gauge area reduces by a factor of 4. This option has the additional advantage of that output voltage is not reduced.

For solving the second problem, the end of each LDT and the reception corner of each hinge attachment were made in a circular shape with a radius of 0.125mm (see Fig. 1.2). This type of arrangement will significantly reduce the lack of fit.

LDTs of required dimensions (65mm x 3.5mm x 0.25mm) were cut out of a thin phosphor bronze foil using sparky rod machine very precisely (Fig.1.2 (b)). LDTs were treated with benzene to remove any fat and dirt. Strain gauges were glued at the centre of LDT on both sides symmetrically, Fig. 1.2 (b). Two strain gauges made one arm of the bridge. The strain gauges had a resistance of 120 Ω and were 0.84mm wide and 2.0mm long (Kyowa, KFG-120-2N-C1-16). This type of arrangement theoretically eliminates the error due to change in temperature. Strain gauges were covered with silicon epoxy for water proofing. The bridge was energised using a constant input voltage of 2V. Signal wires from LDTs were taken out of the triaxial cell from a radial hole made in an additional bottom plate. Radial holes were water proofed using glass to metal seals.

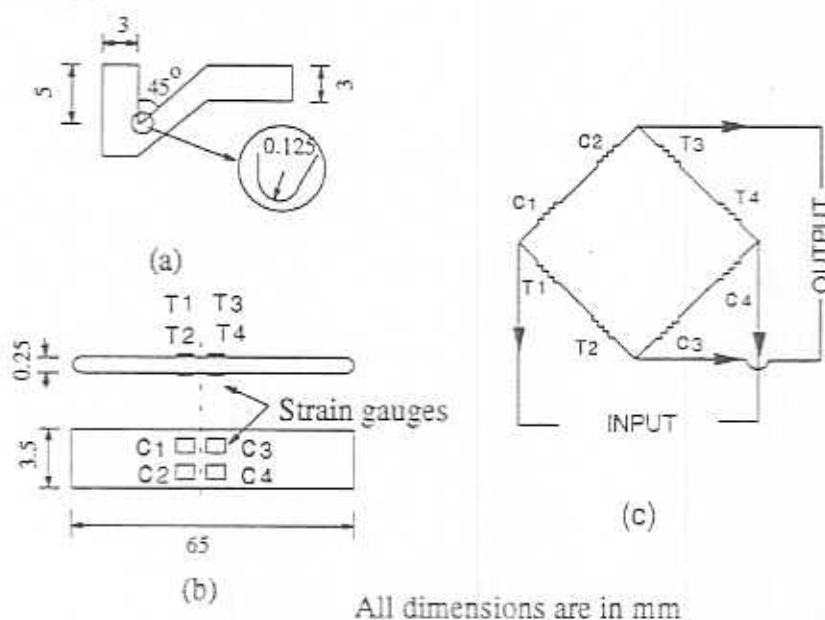


Fig. 1.2. (a) Hinge (b) LDT with strain gauges (c) Wheatstone bridge

1.2.4 Calibration of LDTs

LDTs were calibrated with an Universal Horizontal Metroscope (UHM) of 0.5 micron resolution (readings can be estimated up to 0.1 micron) which corresponds to an axial strain of 7.6×10^{-6} . Measurements with the UHM were made directly by comparing the specimen with a precision glass scale, whose scale divisions were observed through a special spiral microscope. The glass scale was rigidly connected to the measuring spindle. The glass lies in the spindle's longitudinal axis, so that the glass scale necessarily participates in any axial displacement. The displacements were indicated in the microscope and could be read off as measured values. Two cylindrical rods with hinges inside them were mounted on the measuring spindle of UHM. LDTs were inserted in to the cylindrical rods horizontally as shown in Fig. 1.3.

LDTs were calibrated in the air assuming that the presence of water in triaxial cell would not have changed calibration because the Wheatstone bridge is temperature compensating. The wires from the LDTs were connected to a junction box which was connected to the A/D card in the computer. For a small change in displacement, change in voltage is measured from the computer and displacement was measured from the UHM. The calibration experiments were repeated several times incorporating loading, unloading and reloading sequences.

The calibration curves for LDTs are shown in Fig. 1.4. and Fig. 1.5. These curves correspond to various calibration tests, some tests carried out after a few triaxial tests. The scatter mainly attributed to signal noise, hysteresis of LDTs, imperfect-alignment of LDTs in hinges and possibly a small drift in strain gauge position due to insufficient heat dissipation.

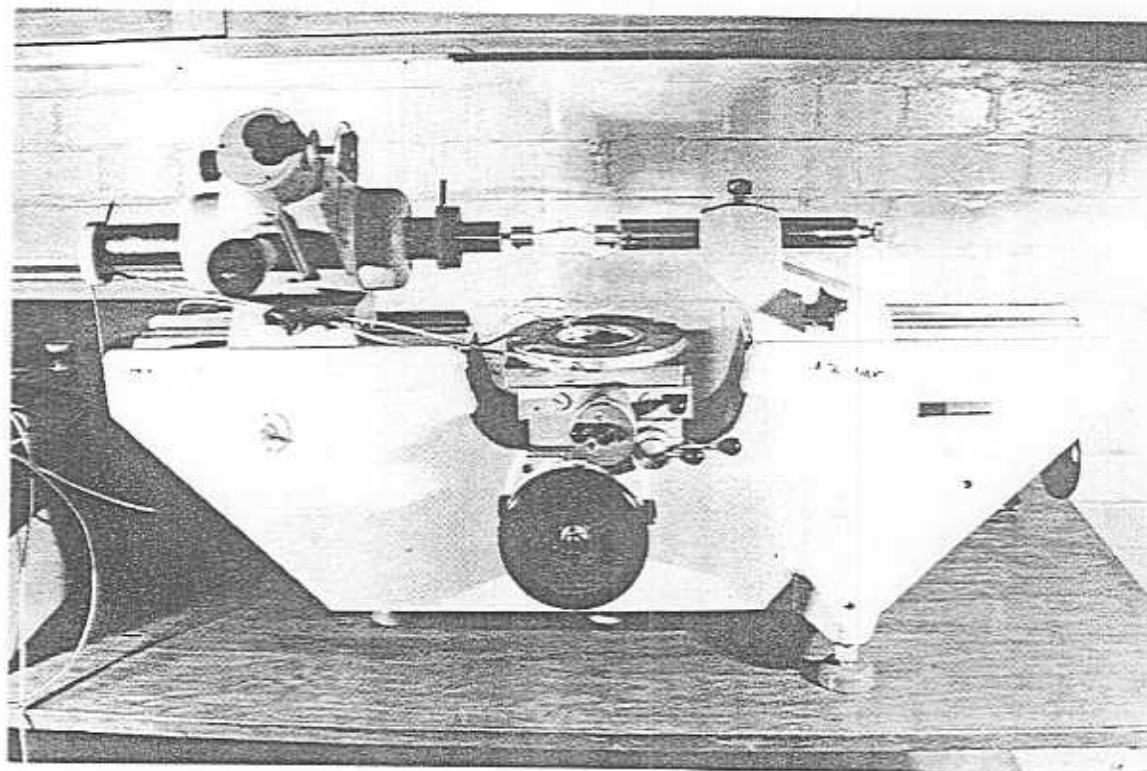


Fig. 1.3 Universal Horizontal Metroscope with LDTs

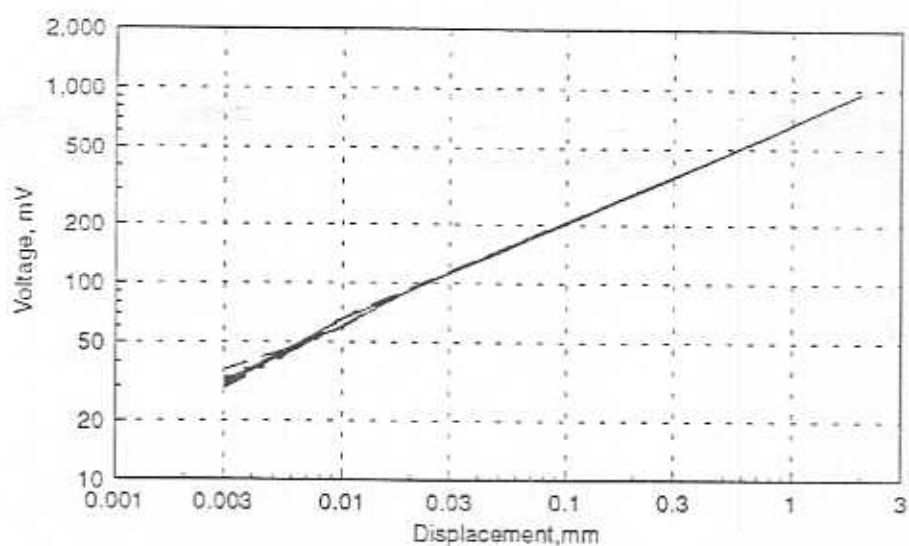


Fig. 1.4 Calibration curves for LDT1 includes loading, unloading and reloading sequences

1.2.5 Signal noise, Resolution and Accuracy of LDTs

(a) Electrical noise

In the present system, electrical noise mainly comes from the A/D card, amplifier in junction box and variations in input voltage. Fig. 1.6 shows the signal noise generated by A/D card and noise in input voltage for channel 2. This is recorded by short circuiting the channel on A/D card and using F200 filter. There is signal noise of about 0.15 mV (it was 3 mV when F0 was used). Fig. 1.7 shows the signal noise with A/D card, junction box and LDT. This is recorded with LDTs connected but stationary. Noise level increased up to 0.7 mV (it was 6 mV when F0 was used) because of amplifier and input voltage variations. LDTs kept in a temperature controlled room for a day showed maximum variation of 1 mV. This is the total electrical noise in the signal that can be expected in the present set-up.

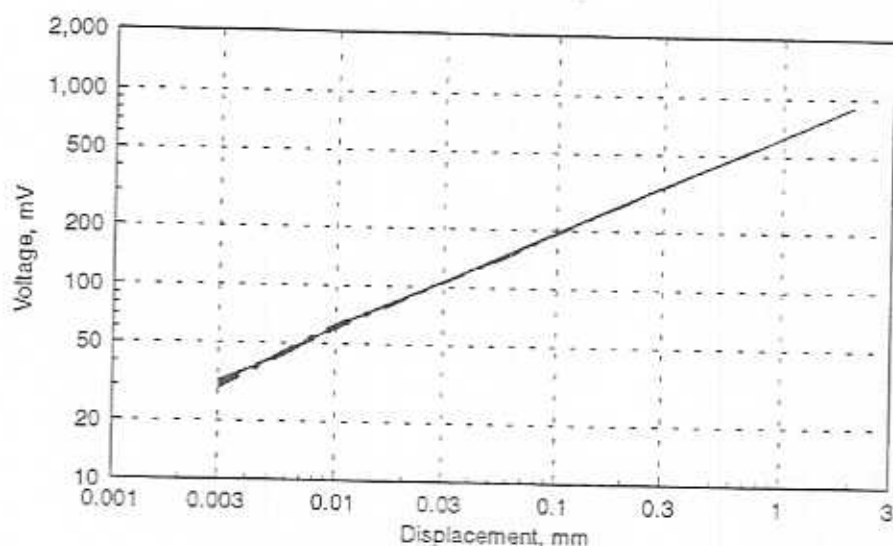


Fig. 1.5 Calibration curves for LDT2 includes loading, unloading and reloading sequences

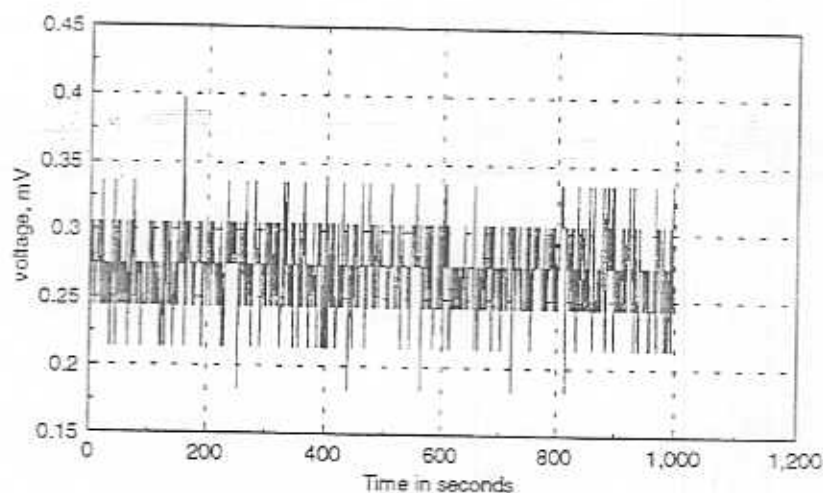


Fig. 1.6 Signal noise due to variations in input voltage and A/D card

(b) Mechanical noise

The final calibration curves (Fig. 1.4 and 1.5) showed more noise than the electrical noise. There is maximum difference of equal to 6 mV at the beginning and about 3 mV towards the

end among various calibration curves. This is quite high compared to the electrical noise. This additional noise is due to hysteresis of LDTs, imperfect alignment of LDTs during calibration and the slight irregularities in mechanical contact (improved by making LDT edges and hinges smooth and of same radius).

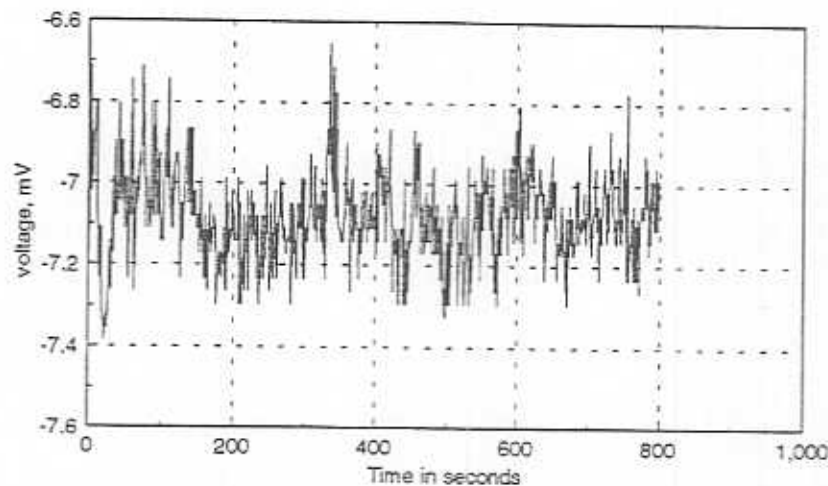


Fig. 1.7 Signal noise due to A/D card and amplifier in junction box

c) Resolution and Accuracy

The resolution of logging system, with 16 bits A/D card and input voltage range of $\pm 1V$, is ± 0.0305 mV. The calibration curves for LDT2 (Fig. 1.5) show that 2mm axial movement causes 900 mV change. Therefore the average resolution of the LDT2 is 6.7×10^{-5} mm. This is equivalent to an axial strain of 8.6×10^{-7} for a 76mm soil sample. The resolution of the LDTs is very high at the beginning than this average value. This is the resolution of the system but not the accuracy! The calibration equation for LDT2 (up to 0.75 mm displacement) is given by

$$\Delta = 2.352V^2$$

where

Δ is displacement in mm

V is voltage in Volts.

Differentiation of the above equation is

$$d\Delta = 4.704VdV$$

Therefore, the accuracy of the LDT is a function of total voltage (strain) as well as noise in voltage. As noted above, for the maximum electrical noise of 1.0 mV, the noise in displacement at 100 mV is 0.00047 mm which corresponds to an axial strain of 6.03×10^{-6} . But at 500 mV, it is 3×10^{-5} . So LDTs are accurate up to at least 3×10^{-5} up to 500 mV. This is from electrical signal noise only.

Total noise (mechanical and electrical) was observed to be 6 mV at the beginning and 3 mV towards the end. For a 6 mV noise at the beginning the accuracy is 4×10^{-5} and towards the end at 500 mV it is 9×10^{-5} beyond which high accuracy is not necessary. So LDTs accuracy is function of strain itself!

1.2.6 Improving the accuracy of LDTs

As shown above the noise is due to (a) mechanical imperfections (b) amplification (c) hysteresis of LDTs and (d) variations in input voltage. The noise from mechanical system is about 6 mV which corresponds to 0.003 mm. It is very unlikely that a mechanical system can be improved more than 3 microns accuracy. The noise from amplifier in junction box and A/D card is small compared to the former. The noise from the A/D card can be reduced by more accurate and noise free A/D cards. The noise from the amplifier may be reduced by using filters. An Fast Fourier Transformation (FFT) on the signal from LDTs showed that the noise is at low frequencies (0.05 Hz). A low frequency filter should replace the general purpose filter adopted in the junction box. Unfortunately, both the options were deemed to be expensive, so it was decided not to further modify the set-up.

1.2.7 Fixing device

The initial near perfect attachment is very important. During calibration it was observed that the initial straightness can effect the results. The hinges are attached to the soil sample using the fixing device, Fig. 1.8. Using the fixing device LDTs can be fixed to soil sample straight and with a given initial curvature.

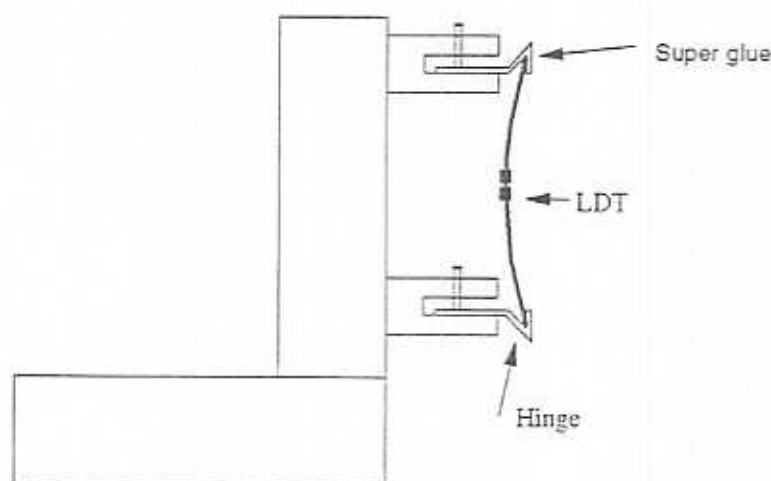


Fig. 1.8. Fixing device used to connect LDTs to soil sample

1.2.8 Extension cap

An extension cap was added to the set-up to carry out extension and cyclic tests. Various methods have been designed and adopted (Head, 1986) but a simpler suction cap modified by Ng (1992) was used, Fig. 1.9.

1.3 Small Strain Measurement

The modified set-up has been used to measure the small strain stiffness of Gault Clay obtained from Madingley site, Cambridge. The Gault Clay in its natural state is heavily overconsolidated, having natural water content close to its plastic limit. The samples were obtained from 2 - 3m deep layers. The Gault Clay in the Cambridge area has been reported by Worssam and Taylor (1975) to contain calcium carbonated up to 30% by weight. Powell and Butcher (1991) reported the small strain stiffness of Gault Clay at Madingley obtained from geophysical measurements. There seems to be good agreement between the stiffness obtained from geophysical methods and laboratory triaxial test results when axial strains are measured by internal gauges (Ng et al., 1995). A detailed analysis of stiffness comparisons from various methods is given in Dasari (1995).

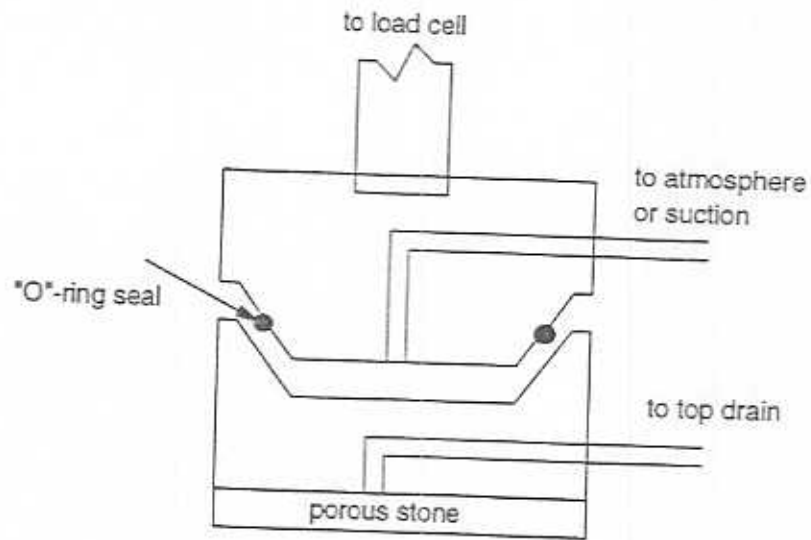


Fig. 1.9 Extension Cap

1.3.1 Calibration curves for load cell and LVDTs

The calibration curves for load cell and LVDTs are shown in Fig. 1.10 and 1.11. To find the

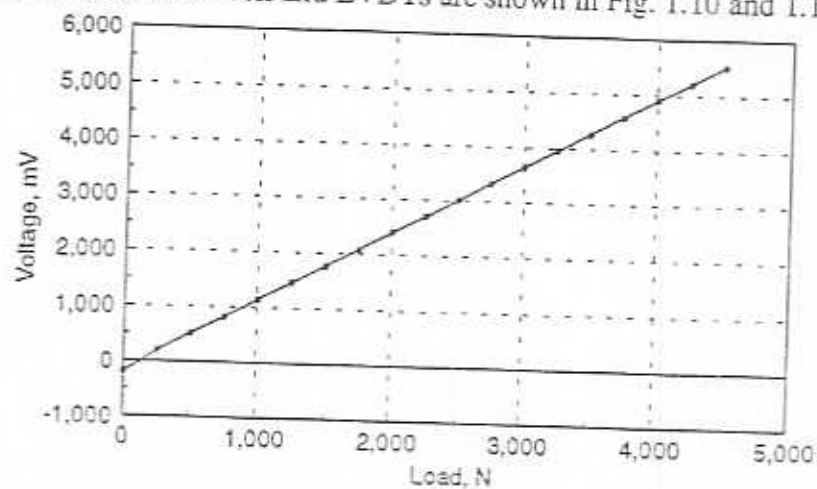
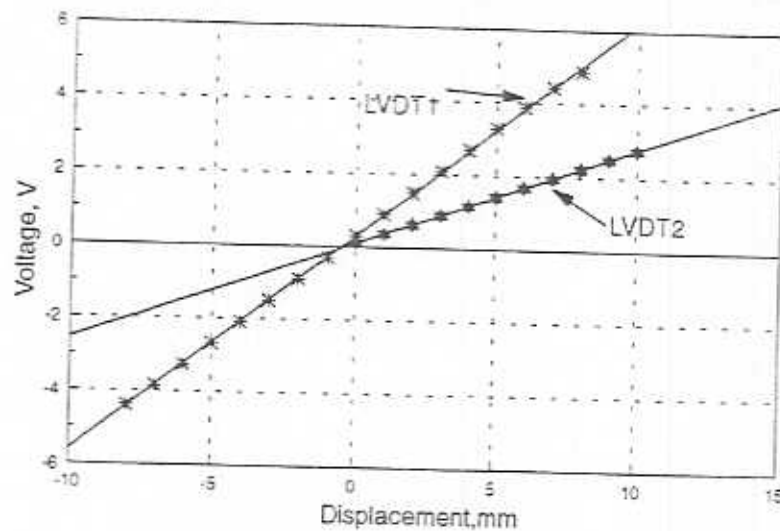


Fig.1.10 Calibration curve for load cell



load cell deflection characteristics an experiment with an aluminium sample placed in triaxial was conducted. Aluminium sample has very flat ends so that errors due to bedding can be assumed to be zero. The axial displacement of aluminium sample was measured using LDTs. Total deflection was measured using LVDTs. The deflection of the load cell is calculated as the difference of average of LVDTs and LDT reading. The deflection of load cell is shown in Fig. 1.13. For a 500 kPa deviatoric stress load cell deflection is about 0.3 mm which corresponds to 0.25% axial strain. In extension, load cell seems to be less stiffer than in compression.

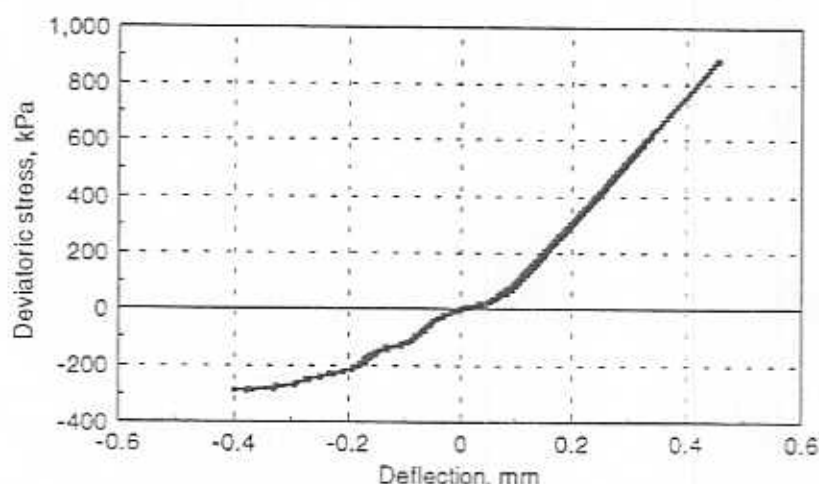


Fig. 1.12 Deflection of load cell for slow cyclic loading

1.3.2 Sample set-up

Soil samples of 38mm x 76mm size were carefully extracted from 38mm diameter samplers. Soil sample was placed with flat edges (to avoid bedding error) on the pedestal. Hinges were attached using fixing device to the membrane of the soil sample using super glue. As shown in Fig. 1.13, two centrally strain gauged LDTs were inserted in to hinges. The distance between the two hinges was slightly shorter than the length of the strip so that, when the strip was mounted, it balances itself, by its own elastic force, against the fixed attachments. In the present study LDTs were attached with an initial 1.0 mm displacement. This ensures that after the soil has swelled back during saturation, LDTs will have an initial displacement of less than 0.5mm before the commencement of shear.

1.3.3 Saturation

Sample was initially saturated at a cell pressure of 200 kPa and a back pressure of 100 kPa. After every 2 days the cell pressure and back pressure were increased, such that final cell pressure was 100 kPa away from the p' corresponding to beginning of the test. A minimum back pressure of 200 kPa was adopted. The full saturation process took about two weeks. The value of 'B' adopted for saturation was 0.75 - 0.8. For a fully saturated soft soils 'B' is close to 1.0, but for fully saturated stiff overconsolidated clays it is less than 1.0 (Black and Lee, 1973 and Head, 1986). In the following section an attempt was made to estimate the value of 'B' for 99% saturation of the Gault Clay soil sample.

1.3.4 Value of B at 99% saturation for Gault Clay

Let us consider a soil matrix of unit gross volume with pore fluid. Let K_s , K_f be the bulk stiffness of soil and fluid respectively. For an increase in all round pressure Δp , the increase in pore pressure is Δu , then

1.3.4 Value of B at 99% saturation for Gault Clay

Let us consider a soil matrix of unit gross volume with pore fluid. Let K_s , K_f be the bulk stiffness of soil and fluid respectively. For an increase in all round pressure Δp , the increase in pore pressure is Δu , then

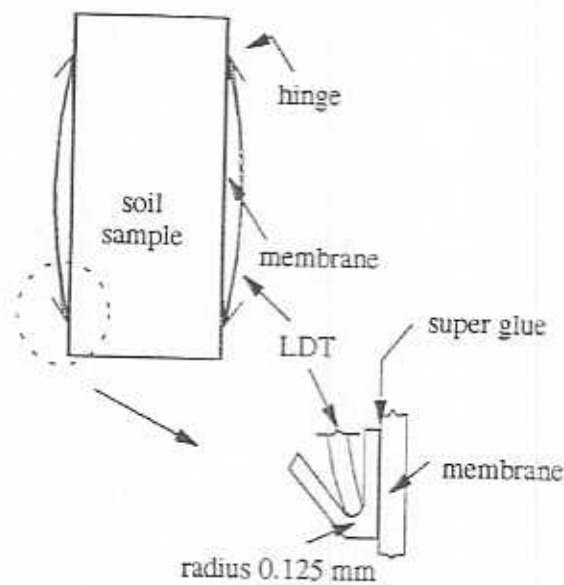


Fig. 1.13 LDTs connected to soil sample

$$\Delta u = B \Delta p \quad (1)$$

$$\Delta p' = (1-B) \Delta p \quad (2)$$

$$\epsilon_v = \delta v = \frac{nB\Delta p}{K_f} = \frac{(1-B)\Delta p}{K_s} \quad (3)$$

where

B is saturation coefficient

ϵ_v is volumetric strain

δv is change in volume

n is porosity of soil

It follows from above equation that

$$B = \frac{1}{1 + n(K_s/K_f)} \quad (4)$$

and bulk modulus of fluid (pore water + pore air) can be shown as

$$K_f = \frac{1}{(1/K_w) + (1 - S_r)/u} \quad (5)$$

where

K_w is bulk modulus of water

S_r is degree of saturation

u is pore pressure

Let us take following properties

$K_s = 30000$ kPa (average stiffness for an increase of 50 kPa, which is used for B test)

$K_w = 2 \times 10^6$ kPa

The value of B from above equations is 0.56. These calculations assume that no appreciable amount of additional pore air would dissolve in to the pore water. The ' B ' values for different types of soils given by Black and Lee (1973) are presented in Table 2. Therefore, it is assumed that the observed value of B 0.7 - 0.8 soil is saturated more than 99%.

Table 2. ' B ' Values For Different Types of Soil at Complete and Nearly Complete Saturation (after Black and Lee, 1973)

| Class of Soil (stiffness of soil) | Saturation = 100% | Saturation = 99.5% | Saturation = 99% |
|--------------------------------------|----------------------|-----------------------|---------------------|
| Soft (N.C. Clays) (700 kPa) | 0.9998 | 0.992 | 0.986 |
| Medium stiff (7000 kPa) | 0.9988 | 0.963 | 0.930 |
| Stiff (70000 kPa) | 0.9877 | 0.69 | 0.51 |
| Very Stiff (700000 kPa) | 0.913 | 0.20 | 0.10 |

1.3.5 Results from a test

Results of a triaxial test conducted on Gault Clay from Madingley site are presented. Test was a slow cyclic drained constant p' ($p'=100$ kPa), carried out using continuous linear stress paths by volume control. The stress path followed was ABCDE and the resultant stress-strain curve for loading, unloading and re-loading is shown in Fig. 1.14. The stiffness-strain curve for loading (BC) and re-loading (DE) is shown in Fig. 1.15. As expected, stiffness due to 180° rotation (DE) is higher than 90° rotation (BC).

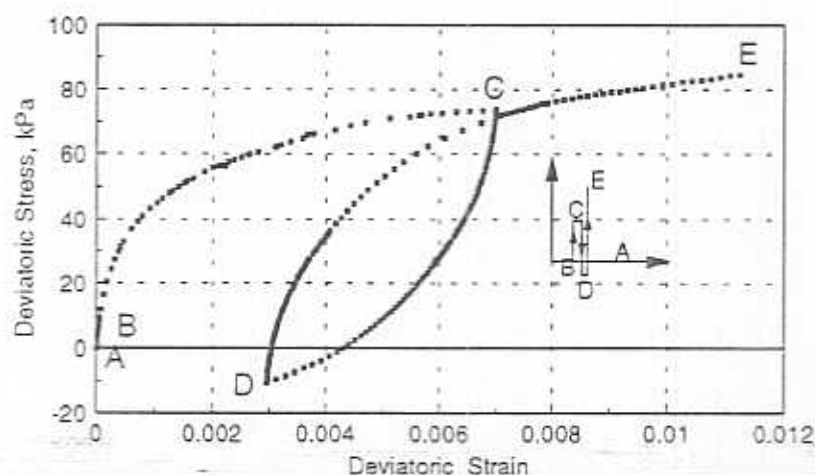


Fig. 1.14 Deviatoric stress-strain curve of Gault Clay at $p'=100$ kPa

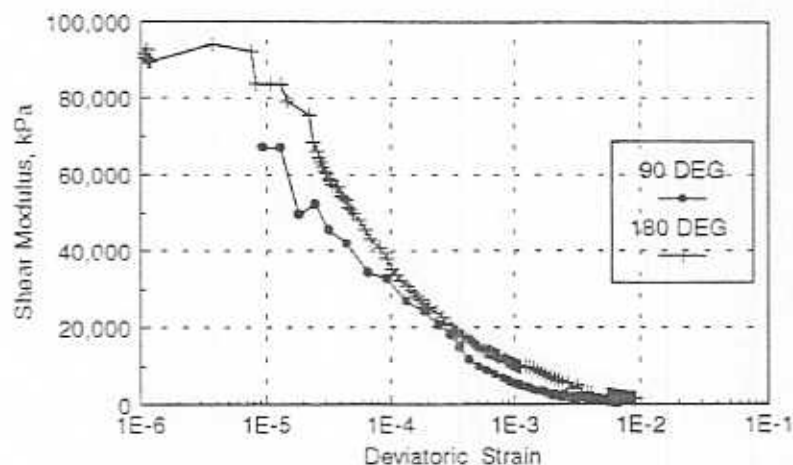


Fig. 1.15 Stiffness-strain curve of Gault Clay from Madingley site

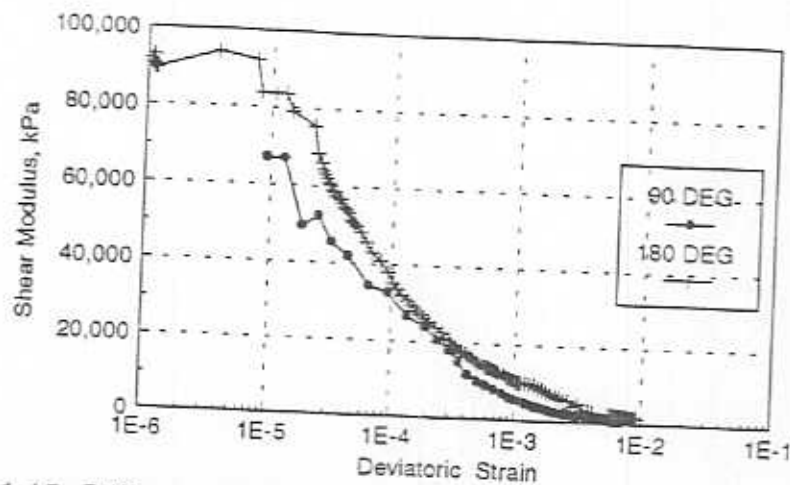


Fig. 1.15 Stiffness-strain curve of Gault Clay from Madingley site

1.4 Discussion

Measurement of axial strain can be improved using LDTs. The accuracy of the measurements depends on electrical and mechanical noise in the system, as explained in section 1.2.6. It is observed that mechanical noise was higher than electrical noise. The increased number of strain gauges and rounding the corners of LDTs and hinges, increased the accuracy of the system. The resolution of the LDTs with ± 1 Volt range on a 16 bit A/D card is about 8×10^{-7} but the accuracy is found to be approximately 4×10^{-5} . Another important factor which effect the accuracy was the discrepancy between two LDTs readings. A typical curve with LDT1 and LDT2 readings is shown in Fig. 1.16. As shown, below 5×10^{-5} strain readings are scattered though on average results look all right. Therefore the accuracy of the measurements using LDTs is about 5×10^{-5} .

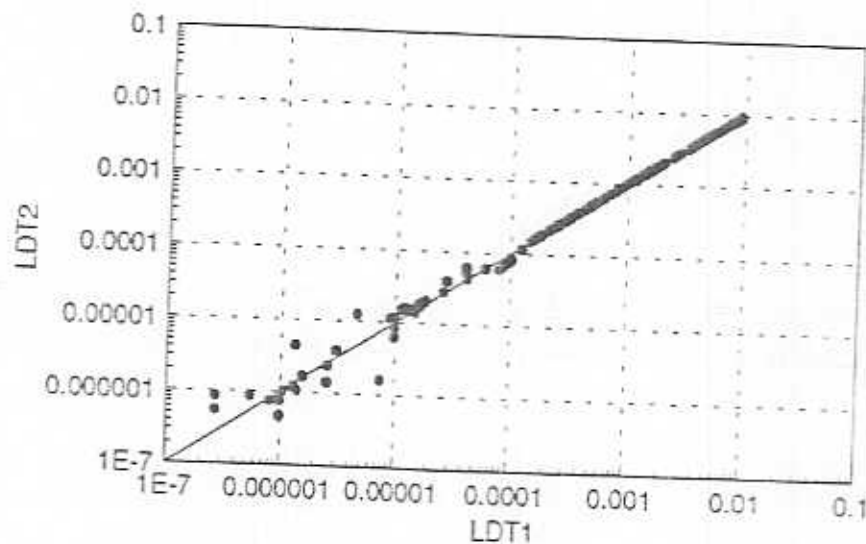


Fig. 1.16 LDT1 Vs LDT2 readings for a constant p' test

The radial strains calculated from volumetric controller are another source of error. Although the accuracy of the volume controller was about 1×10^{-5} , the assumption of right cylinder deformation is open to discussion. Therefore, it is necessary to measure the radial strains externally may be using a circular LDT attached to soil sample at mid height.

1.5 Adding New Internal Gauges

New internal gauges can be added to the system as given in Table 1. ADTINI program should be used to initialise the new internal gauge. Select appropriate voltage on A/D card and

REFERENCES

1. Abbiss, C.P. (1981). Shear wave measurements of the elasticity of the ground. *Geotechnique*, Vol. 31, No.1, pp.91-104.
2. Arthur, J.R.F. and Phillips, A.B. (1975). Homogeneous and layered sand in triaxial compression. *Geotechnique*, Vol. 25, No.4, pp.799-815.
3. Balasubramanian, A.S. (1976). Local strains and displacement patters in triaxial specimens of a saturated clay. *Soils and Foundations*, Vol.16, No.1, pp.101-114.
4. Baldi, G., Hight, D.W., Thomas, G.E. (1988). A reevaluation of conventional triaxial test methods. *Advanced Triaxial Testing of Soil and Rock*, ASTM STP 977, pp.219-263.
5. Black, D.K. and Lee, K.L. (1973). Saturating laboratory samples by back pressure. *Jl of SMFE, ASCE*, Vol.99, No.SM1, pp.75-93.
6. Bolton, M.D., Sun, H.W. and Britto, A.M. (1993). Finite element analyses of bridge abutments on firm clay. *Computers and Geotechnics*, Vol.15, No.4, pp.221-245.
7. Bolton, M.D., Dasari, G.R. and Britto, A.M. (1994). Putting samll strain non-linearity into Modified Cam Clay model. *Proc. of 8th IACMAG*, Siriwardane and Zaman (eds.), Morgantown, West Virginia, USA, pp.537-542.
8. Brown, S.F., Austin, G. and Overy, R.F. (1980). An instrumented triaxial cell for cyclic loading of clays, *Geotechnical Testing Jl., ASTM*, Vol.3, No.4, pp.145-152.
9. Burland, J.B. and Symes, H.J.R.P. (1982). A simple displacement gauge for use in triaxial apparatus, *Geotechnique*, Vol.32, No.1, pp.62-64.
10. Clayton, C.R.I. and Kathrush, S.A. (1986). A new device for measuring local axial strains on triaxial specimen. *Geotechnique*, Vol.36, No.4, pp.593-597.
11. Clayton, C.R.I., Kathrush, S.A., Bica, B.V.D. and Siddique, A. (1989). The use of hall effect semi-conductors in geotechnical instrumentation, *Geotechnical Testing Jl., ASTM*, Vol.12, No.1, pp.69-76.
12. Clayton, C.R.I, Gordon, M.A. and Matthews, M.C. (1994). Measurement of stiffness of soils and weak rocks using small strain laboratory testing and field geophysics. *Pre-failure Deformation of Geomaterials*, Shibuya , Mitachi and Miura (eds), Sapporo, Japan, pp. 229-234.
13. Costa-Filho, L.de M. (1985). Measurement of axial strains in triaxial tests on London clay, *Geotechnical Testing Jl., ASTM*, Vol.8, No.1, pp.3-13.
14. Dasari, G.R. (1995). The importance of modelling of small strain stiffness on movements due to Tunnelling and Diaphragm walls. PhD thesis to be submitted to University of Cambridge.
15. Dyvik, R. and Oslen, T.S. (1989). G_{max} measured in Oedometer and DSS tests using bender elements, *Proc. of the 12th Int. Conf. on SMFE*, Rio de Janeiro, Vol.1, pp.39-42.
16. Goto, S., Tatsuoka, F., Shibuya, S., Kim, Y.S. and Sato, T. (1991). A simple gauge for local small strain measurements in the laboratory. *Soils and Foundations*, Vol.31, No.1, pp.169-180.
17. Hardin, B.O. and Drenevich, V.P. (1972). Shear modulus and damping of in soils. Measurement and parameter effects, *Jl. of SMFE, Proc. of ASCE*, Vol.98, No. SM6, pp.603-624.
18. Head, K.H. (1986). *Manual of soil laboratory testing*. Volume 1,2 and 3. Pentech Press, London.
19. Hird, C.C. and Yung, P.C.Y. (1989). The use of proximity transducers for local strain measurements in triaxial tests, *Geotechnical Testing Jl., ASTM*, Vol.12, No.4, pp.292-298.
20. Jardine, R.J., Symes, M.J. & Burland, J.B. (1984). The measurement of soil stiffness in the triaxial apparatus. *Geotechnique*: 34, 323-340.
21. Jardine, R.J., Potts, D.M., Fourie, A.B. and Burland, J.B. (1986). Studies of the influence of non--linear stress--strain characteristics in soil--structure interaction, *Geotechnique*, 36: 377-396.

16. Goto, S., Tatsuoka, F., Shibuya, S., Kim, Y.S. and Sato, T. (1991). A simple gauge for local small strain measurements in the laboratory. *Soils and Foundations*, Vol.31, No.1, pp.169-180.
17. Hardin, B.O. and Drenevich, V.P. (1972). Shear modulus and damping of in soils. Measurement and parameter effects, *Jl. of SMFE, Proc. of ASCE*, Vol.98, No. SM6, pp.603-624.
18. Head, K.H. (1986). *Manual of soil laboratory testing*. Volume 1,2 and 3. Pentech Press, London.
19. Hird, C.C. and Yung, P.C.Y. (1989). The use of proximity transducers for local strain measurements in triaxial tests, *Geotechnical Testing Jl., ASTM*, Vol.12, No.4, pp.292-298.
20. Jardine, R.J., Symes, M.J. & Burland, J.B. (1984). The measurement of soil stiffness in the triaxial apparatus. *Geotechnique*: 34, 323-340.
21. Jardine, R.J., Potts, D.M., Fourie, A.B. and Burland, J.B. (1986). Studies of the influence of non-linear stress-strain characteristics in soil-structure interaction, *Geotechnique*, 36: 377-396.
22. Kokush, T. (1980). Cyclic triaxial test of dynamic soil properties for wide strain range, *Soils and Foundations*, Vol. 20, No.2, pp.45-60.
23. Lacasse, S. and Berre, T. (1988). Triaxial testing methods for soils, S-O-A Paper, ASTM STP 977, *Advanced Triaxial Testing of Soil and Rock*, pp 264-289.
24. Lefebvre, G., Leboeuf, D., Rahhal, M.E., Lacroix, A., Warde, J. and Stokoe II, K.H. (1994). Laboratory and field determinations of small-strain shear modulus for a structured Champlain clay. *Canadian Geotechnical Jl., Vol., 31*, pp.61-70.
25. Ng, C.W.W.N. (1992). An Evaluation of Soil-structure interaction associated with a multi-propped excavation, PhD thesis, University of Bristol, UK.
26. Ng, C.W.W.N., Bolton, M.D. and Dasari, G.R. (1995). The small strain stiffness of a carbonate stiff clay. Technical note accepted for publication in *Soils and Foundations*.
27. Simpson, B., O'Riordan, N.J. & Croft, D.D. (1979). A computer model for the analysis of ground movements in London clay. *Geotechnique*, 29:149-175.
28. Simpson, B. (1992). Thirty-second Rankine Lecture: Retaining structures: displacement and design. *Geotechnique*, 42, 541-576.
29. Stallebrass, S.E. (1990). Modelling the effect of recent stress history on the deformation of overconsolidated soils. PhD thesis, City University, London.
30. Taylor, P.W. and Parton, I.M. (1973). Dynamic torsion testing of soils. *Proc. of the 8th Int. Conf. on SMFE, Moscow*, Vol. 1, Paper No.65, pp.425-432.
31. Viggiani, G. (1992). Small strain stiffness of fine grained soils, PhD thesis, City University, London.
32. Worssam, B.C. and Taylor, J.H. (1975). *Geology of the country around Cambridge*. 2nd edition. Her Majesty's Stationery Office, London.
33. Yasuda, N. and Matsumoto, N. (1994). Comparisons of deformation characteristics of rockfill materials using monotonic and cyclic loading laboratory tests and in situ tests. *Canadian Geotech. Jl., Vol.31*, pp. 162-174.